Journal of Aerospace Engineering, Volume 37, Issue 2, March 2024, Article number 5250
DOI:10.1061/JAEEEZ.ASENG-5250

Analytic Approach for Impact Time Guidance with Look Angle Constraint Using Exact Time-to-Go Solution

Seokwon Lee [1], Jinrae Kim [2], Youdan Kim[3], and Namhoon Cho[4]

ABSTRACT

This paper proposes an analytic approach for impact-control guidance laws against stationary targets using biased proportional navigation. The proposed guidance scheme realizes the impact time control in two different ways: the first approach directly uses the exact time-to-go error to satisfy both the impact-time-control and the field-of-view constraint, while the second approach adopts a look angle tracking law to indirectly control the impact time, with the reference profile of the look angle generated using the exact time-to-go solution. The stability properties of the proposed guidance laws are discussed, and numerical simulations are carried out to evaluate their performance in terms of accuracy and efficiency.

1 INTRODUCTION

Impact time control (ITC) has been a subject of interest in guidance systems for decades. ITC involves completion of the engagement at a specific time, and its importance was initially recognized in anti-ship missile systems for enhancing attack effectiveness and survivability through time-coordination strategies such as salvo attack and sequential strike (Jeon et al. 2010; Zhang et al.

[1]Assistant Professor, Department of Mechanical Engineering, Chung-Ang University, Seoul, 06974, Republic of Korea, (corresponding author, e-mail:seokwonlee@cau.ac.kr)

[2]Ph D Candidate, Department of Aerospace Engineering, Seoul National University, Seoul, 08826, Republic of Korea. (e-mail:kjl950403@snu.ac.kr)

[3]Professor, Department of Aerospace Engineering, The Institute of Advanced Aerospace Technology, Seoul National University, Seoul, 08826, Republic of Korea. (e-mail:ydkim@snu.ac.kr)

[4]Research Fellow, Centre for Autonomous and Cyber-Physical Systems, School of Aerospace, Transport, and Manufacturing, Cranfield University, Cranfield, MK43 0AL, United Kingdom. (e-mail:n.cho@cranfield.ac.uk)

Published by ASCE. This is the Author Accepted Manuscript issued with: Creative Commons Attribution Non-Commercial License (CC:BY:NC 4.0).
The final published version (version of record) is available online at DOI:10.1061/JAEEEZ.ASENG-5250. Please refer to any applicable publisher terms of use.

2020; Tahk et al. 2018; Li and Ding 2018). Moreover, the concept of ITC has been extended to simultaneously consideration of the impact angle (Lee et al. 2007; Harl and Balakrishnan 2012; Kim et al. 2013; Harrison 2012; Livermore and Shima 2018; Hu et al. 2018) and seeker‘s field-of-view (FOV) limit (Sang and Tahk 2009; Tekin et al. 2016; Zhang et al. 2014; Chen and Wang 2018; Kim and Kim 2019; Erer and Tekin 2016; Jeon and Lee 2017; Tekin et al. 2017a; Tekin et al. 2017b; Tekin and Erer 2020; Kim et al. 2020; Saleem and Ratnoo 2016; Wang et al. 2019; Tsalik and Shima 2019; Lee et al. 2020; Dong et al. 2022; Kang et al. 2023a).

Recent research has considered the seeker's field-of-view (FOV) limit in the design of ITC. The FOV limit restricts the missile's maneuverability to maintain its look angle within a predefined FOV consistently. Studies on ITC with a look angle constraint can be broadly classified into two categories. The first category involves directly handling the impact time error in terms of time-to-go while ensuring the look angle constraint is met. Biased proportional navigation guidance (BPNG) have been widely adopted to regulate the impact time error by means of ITC (Sang and Tahk 2009; Tekin et al. 2016; Lee et al. 2020; Zhang et al. 2014; Kim et al. 2021; Cho and Lee 2021; He et al. 2020). Sang and Tahk (Sang and Tahk 2009) proposed a switching framework to cope with the FOV constraint, while Tekin et al. (Tekin et al. 2016) analyzed the range of achievable time with respect to the FOV constraint. Zhang et al. (Zhang et al. 2014) proposed an impact-time-control guidance law using BPNG and an approximate model to generate the impact time error. He et al. (He et al. 2020) designed the impact-time control guidance (ITCG) via optimal error feedback formulation.

The second category involves designing the ITCG using an indirect controlled variable in terms of look angle error, rather than time-to-go error. Two approaches have been employed in this category: trajectory shaping guidance and reference-tracking type guidance (Jeon and Lee 2017; Tekin et al. 2017a; Tekin et al. 2017b; Tekin et al. 2018; Tekin and Erer 2020; Kim et al. 2020; Kim et al. 2021). In the trajectory shaping approach, the guidance law is designed by shaping the trajectory to satisfy multiple constraints expressed as polynomials of variables such as range and look angle. The terminal time and FOV constraints are satisfied by appropriately

selecting the coefficients of the polynomials, and the guidance command is generated to follow the trajectory profile. In general, the trajectory shaping methods include online optimization process to select the coefficients. For impact time control problem, total path length and FOV limit are imposed as equality and inequality constraints, respectively. The parameter selection process is then formulated as a parametric optimization problem, which may require additional computation. In the reference-tracking type approach, a reference is designed to satisfy boundary conditions such as impact time and look angle constraints. An error feedback routine is then incorporated to control the variable and follow the reference. While these approaches offer advantages in shaping the guidance trajectory while satisfying the constraints, they essentially follow an open-loop control procedure and are sensitive to performance errors due to uncertainties.

In both approaches, accurate time-to-go information is crucial for achieving ITC and ensuring precise timing coordination and control. The time-to-go information is used to measure the remaining time and impact time error and is incorporated directly or indirectly in the ITC. However, obtaining the time-to-go information through nonlinear control schemes (Kim et al. 2015; Kumar and Ghose 2015; Cho et al. 2016; Kim et al. 2019a; Hu et al. 2019) can be challenging, as closed-loop kinematics must be solved exactly. Some research works modified the PNG by varying the navigation gain, which leads to obtain solvable closed-loop kinematics and reduce computational burden (Dong et al. 2023; Kang et al. 2023b). On the other hand, ITC schemes based on proportional navigation guidance (PNG) (Jeon et al. 2006; Cho and Kim 2016) have been found useful in obtaining the time-to-go solution, as the guided trajectory can be obtained in closed form. Nevertheless, the accuracy of existing methods for time-to-go calculation is limited by the use of approximate solutions (Tahk et al. 2018; Ryoo et al. 2006; Dhananjay and Ghose 2014), which can degrade performance in explicit time-to-go guidance laws. In both direct and indirect impact time control approaches, guidance laws are often designed using linearized engagement kinematics (Jeon et al. 2006) or approximate time-to-go forms (Zhang et al. 2014; He et al. 2020), leading to unsatisfactory performance due to inaccuracies in the relationship between time-to-go and control variables.

This study presents an analytic approach to design guidance laws for ITC, where an exact time-to-go solution is derived for precise impact time error. Motivated by the previous studies (Cho and Kim 2016; Kim et al. 2021), the study designs BPNG laws that satisfy the look angle constraint while maintaining PNG performance. A pure proportional navigation guidance (PPNG) serves as a baseline guidance law, and the exact time-to-go solution is used to accurately track ITC. The study introduces an additional bias input to compensate for the impact time error, and various error variables can be chosen to design the bias command. The proposed guidance laws are suitable for two ITCG approaches: explicit time-to-go error regulation and feedback law synthesis, and control of impact time through the tracking of the reference look angle profile. Lyapunov stability theory is used to investigate error convergence and positive invariance of the look angle solution. The study also includes discussions on guidance law design guidelines, and similarities and comparisons between the proposed guidance laws.

This study makes several contributions. Firstly, the proposed analytic approach utilizes exact time-to-go solutions, resulting in more accurate impact time control compared to existing methods that rely on approximate time-to-go formulas. The use of analytic solutions enables designers to effectively analyze the guidance laws and significantly improve performance, particularly near the interception moment. Secondly, the proposed methods are designed using the BPNG framework, which preserves the benefits of the BPNG technique. The BPNG approach handles impact time error and look angle constraints using a bias input, while the PNG is used for intercept capability during the terminal phase. Both proposed guidance laws comply with the BPNG structure and utilize its features. Thirdly, the proposed guidance laws generate continuous inputs, resulting in more stable performance than the existing two-stage guidance laws (Sang and Tahk 2009; Lee et al. 2020). Finally, comparative discussion provides insight into possible variations of the BPNG design for ITCG.

2 PROBLEM FORMULATION AND PRELIMINARIES

In this section, the equations of motion for the missile and target are described in Sec. 2.1. The guidance objective considered in this study is then described in Sec. 2.2.

2.1 Equations of Motion

Consider the planar motion of a missile with respect to a stationary target as shown in Fig. 1. The following assumptions are used throughout this study.

Assumption 1. The interceptor is considered as a lag-free vehicle maintaining a constant speed.

Assumption 2. The angle of attack is negligible.

The look angle is defined as

$$\sigma = \gamma - \lambda \tag{1}$$

where γ is the flight-path angle of the missile. λ is the line-of-sight (LOS) angle, respectively. Under Assumption 2, the engagement kinematics can be expressed in polar coordinates as

$$\dot{r} = -V_m \cos\sigma \tag{2a}$$

$$r\dot{\lambda} = -V_m \sin\sigma \tag{2b}$$

$$\dot{\gamma} = \frac{a_m}{V_m} \tag{2c}$$

where r is the distance between the missile and the target. V_m is the speed of the missile. a_m represents the acceleration perpendicular to the velocity vector.

Using Eq. (2) in (1), we have

$$\dot{\sigma} = \frac{V_m}{r}\sin\sigma + \frac{a_m}{V_m} \tag{3}$$

2.2 Problem Definition for impact-time-control

In this section, the problem considered in this study is described according to the design goals. First, this study focuses on the guidance law for target interception at a desired impact time. For instance, the interception must be performed with zero miss distance at the desired impact time. The miss distance in terms of zero-effort-miss can be considered as

$$Z = r\sin\sigma \tag{4}$$

The zero-effort-miss is nullified if σ or r regulate before interception. Note that r strictly decreases if the look angle satisfies

$$\dot{r} = -V_m \cos\sigma < 0 \quad \text{for} \quad |\sigma| < \frac{\pi}{2} \tag{5}$$

Otherwise, the unbounded look angle response increases range and also diverges the guidance command. It is also desirable to regulate the acceleration command in the vicinity of the interception considering the energy-minimization point of view. Note that LOS rate should be zero for stationary target interception. To satisfy both requirements, the terminal condition of σ can be expressed as

$$\dot{\lambda} = -\frac{V_m}{r}\sin\sigma \to 0 \text{ as } r \to 0 \quad \Rightarrow \quad \sigma \to 0 \text{ as } r \to 0 \tag{6}$$

Meanwhile, the look angle should remain consistently within the FOV. The look angle constraint can be expressed as follows:

$$\sigma(t) \in \Sigma = [-\sigma_{\text{lim}}, \sigma_{\text{lim}}], \quad \forall t \in [t_0, t_f] \tag{7}$$

where σ_{lim} is bounded from above by $\pi/2$. The look angle constraint can be achieved if Σ is a positively invariant set and $\sigma(t_0) \in \Sigma$ (Khalil, H. K., and Grizzle 1996). Note that r decreases with respect to time, i.e., Eq.(5), as long as the missile maintains its target inside the seeker's field-of-view for all time, as represented in Eq. (7). In summary, the impact-time-control problem can be stated as follows:

1) (Terminal Condition) The range and the look angle at the impact time must be regulated, i.e., $r \to 0$ and $\sigma \to 0$.
2) (Positive Invariance of Σ, Eq. (7)) The set Σ should be positively invariant. That is, $\sigma(t_0) \in \Sigma \Rightarrow \sigma(t) \in \Sigma, \forall t_0 \le t \le t_f$.
3) (Desired Impact Time) The impact-time error should be less than the allowed value, i.e., $|t_f - t_d| \le \epsilon$, where t_d is a desired impact time.

3 ANALYTIC APPROACH FOR TIME-TO-GO SOLUTION

This section outlines the exact solution of the time-to-go that will be used for designing ITCG laws. The proposed guidance scheme employs the PPNG as the baseline guidance performance. The fundamental characteristics of PPNG are briefly summarized in Section 3.1. Section 3.2 presents the derivation of the time-to-go solution, which is based on the closed-form solution of PPNG.

3.1 Pure Proportional Navigation

The basic principle of the PNG is to steer the vehicle to form a stable collision geometry with the guidance command that is proportional to the LOS rate. In this study, PPNG is considered as a baseline guidance command. The PPNG command is given by (Zarchan 2012)

$$a_{PPNG} = NV_m\dot{\lambda} = -N\frac{V_m^2}{r}\sin\sigma \tag{8}$$

where N is the navigation gain. Using the lateral acceleration generated by the PPNG, i.e., $a_m = a_{PPNG}$, the differential relations of the flight-path angle and look angle can be obtained to be proportional to the LOS angle as

$$\dot{\gamma} = N\dot{\lambda} \tag{9a}$$

$$\dot{\sigma} = \dot{\gamma} - \dot{\lambda} = (N-1)\dot{\lambda} \tag{9b}$$

Using Eqs. (2a), (2b) and (9b), σ and $\dot{\lambda}$ can be evolved with respect to r as

$$\sin\sigma = \sin\sigma_0\left(\frac{r}{r_0}\right)^{N-1} \tag{10}$$

$$\dot{\lambda} = -\frac{V_m\sin\sigma_0}{r_0}\left(\frac{r}{r_0}\right)^{N-2} \tag{11}$$

From Eqs. (10) and (11), the permissible navigation constant satisfying the terminal condition can be expressed as follows: (Shneydor 1998; Zarchan 2012)

1. $\sigma\left(r_f = 0\right) = 0$ if and only if $N > 1$

2. $\dot{\lambda}\left(r_f = 0\right) = 0$ if and only if $N > 2$

3.2 Analytic Solution for Time-to-go

The analytic solution for the time-to-go of the PPNG was derived when the target is stationary (Cho and Kim 2016) and is expressed as a function of N, V_m, r and σ as

$$t_{go,PPN}(r, \sigma; N) = \frac{r}{V_m} \mathcal{F}\left(|\sigma|; N\right) \tag{12}$$

where $\mathcal{F}(|\sigma|; N)$ is defined as

$$\mathcal{F}(|\sigma|; N) \triangleq \begin{cases} {}_2\mathcal{F}_1\left(\frac{1}{2}, \frac{1}{2(N-1)}; 1 + \frac{1}{2(N-1)}; \sin^2\sigma\right) & |\sigma| \leq \frac{\pi}{2} \\ \frac{2}{|\sin\sigma|^{1/N-1}} {}_2\mathcal{F}_1\left(\frac{1}{2}, \frac{1}{2(N-1)}; 1 + \frac{1}{2(N-1)}; 1\right) - {}_2\mathcal{F}_1\left(\frac{1}{2}, \frac{1}{2(N-1)}; 1 + \frac{1}{2(N-1)}; \sin^2\sigma\right) & \frac{\pi}{2} < |\sigma| < \pi \end{cases} \tag{13}$$

The function ${}_2\mathcal{F}_1\left(\frac{1}{2}, \frac{1}{2(N-1)}; 1 + \frac{1}{2(N-1)}; \sin^2\sigma\right)$ can also be expressed as an infinite series:

$${}_2\mathcal{F}_1\left(\frac{1}{2}, \frac{1}{2(N-1)}; 1 + \frac{1}{2(N-1)}; \sin^2\sigma\right) = \sum_{n=0}^{\infty} \frac{(2n)!}{2^{2n}(1 + 2n(N-1))(n!)^2} |\sin\sigma|^{2n} \tag{14}$$

where ${}_2\mathcal{F}_1(a, b; c; z)$ is a Gaussian hyper-geometric function (GHGF) defined as in (Gasper et al. 2004). Note that GHGF is an even function with respect to σ. Because of its symmetricity, the GHGF $\mathcal{F}(|\sigma|; N)$ satisfies

$$\mathcal{F}(|\sigma|; N) \geq 1, \quad \forall |\sigma| \in [0, \pi), \qquad \text{and} \quad \mathcal{F}(0, N) = 1 \tag{15}$$

For the derivation of the partial derivatives, the GHGF for $c = b + 1$ is given by (Cho and Kim 2016; Gasper et al. 2004; Kim et al. 2021)

$$\frac{\partial {}_2\mathcal{F}_1(a, b, b+1; z)}{\partial z} = \frac{b}{z}\left((1-z)^{-a} - {}_2\mathcal{F}_1(a, b, b+1; z)\right) \tag{16}$$

Using the above property, the partial derivative of $\mathcal{F}$ can be obtained as

$$\frac{\partial \mathcal{F}(|\sigma|;N)}{\partial|\sigma|} = \frac{|\cot\sigma|}{N-1}\left(\sec\sigma - \mathcal{F}(|\sigma|;N)\right), \quad \forall\sigma \in (0,\pi) \tag{17}$$

Accordingly, the partial derivative of the time-to-go, $t_{go,PPN}$, given by (12) can be represented as

$$\frac{\partial t_{go,PPN}}{\partial r} = \frac{\mathcal{F}(|\sigma|;N)}{V_m} = \frac{t_{go,PPN}}{r} \tag{18}$$

$$\frac{\partial t_{go,PPN}}{\partial|\sigma|} = \frac{r}{V_m}\frac{|\cot\sigma|}{N-1}\left(\sec\sigma - \frac{V_m}{r}t_{go,PPN}\right) = \frac{1}{N-1}\frac{\left(t_{go,DPP} - t_{go,PPN}\right)}{|\tan\sigma|} \tag{19}$$

where $t_{go,DPP}$ represents the time-to-go of the deviated pure pursuit guidance law (Lee et al. 2020) that can be represented as

$$t_{go,DPP} = \frac{r}{V_m\cos\sigma} \tag{20}$$

Since $t_{go,DPP} - t_{go,PPN} > 0$ for all $\sigma \in \Sigma\backslash\{0\}$, the following properties hold for the partial derivative.

$$\frac{1}{\cos\sigma} > \mathcal{F}(\sigma;N), \quad \text{or} \quad 1 - \cos\sigma\mathcal{F}(\sigma;N) > 0 \tag{21a}$$

$$\frac{\partial t_{go,PPN}}{\partial|\sigma|} \propto \frac{\partial \mathcal{F}(|\sigma|;N)}{\partial|\sigma|} > 0, \quad \forall|\sigma| \in (0,\pi) \tag{21b}$$

$$\lim_{\sigma\to 0}\frac{\partial t_{go,PPN}}{\partial|\sigma|} = \frac{r}{V_m}\lim_{\sigma\to 0}\frac{\partial \mathcal{F}(|\sigma|;N)}{\partial|\sigma|} = 0 \tag{21c}$$

where backlash operator \ indicates the relative complement between sets defined by $A\backslash B = \{x|x \in A, x \notin B\}$ Later, the above properties will be utilized in the ITCG design.

Remark 1. (Approximate Solution of PPNG Time-to-Go) The exact solution of $t_{go,PPNG}$ can be expressed as an infinite series of $\sin^2\sigma$, and it is possible to approximate the solution by taking the first few terms of the series expansion. For example, expansion of the series up to the first order in

$\sin^2\sigma$ gives an approximate expression for the time-to-go as

$$t_{go,approx} \approx \frac{r}{V_m}\sum_{n=0}^{1}\frac{(2n)!}{2^{2n}(1+2n(N-1))(n!)^2}|\sin\sigma|^{2n} = \frac{r}{V_m}\left(1+\frac{\sin^2\sigma}{2(2N-1)}\right) \tag{22}$$

Under small angle assumption, $\sin\sigma \approx \sigma$, it can be further approximated as

$$t_{go,approx,small} \approx \frac{r}{V_m}\left(1+\frac{\sigma^2}{2(2N-1)}\right) \tag{23}$$

Approximate expressions for the time-to-go were used to design guidance laws for the impact-time-control in Refs. (Zhang et al. 2014; He et al. 2020).

Remark 2. (Implementation of the GHGF) The implementation of the exact time-to-go requires calculating the GHGF or the incomplete beta function. Several methods have been developed to ensure efficient and accurate computation, including: i) solving the related differential equation, ii) reading from a table, and iii) using hybrid calculation methods based on the range of input (Pearson 2009). These methods have already been incorporated into numerous software packages designed for implementing special functions (Lozier 2003).

The effectiveness of implementation method was discussed with comparison of time-to-go computation methods (Cho and Kim 2016). It can be observed that the evaluation of the partial sum approximation is slow, and the results are inaccurate. In contrast, the calculation of time-to-go using GHGF or the incomplete beta function show good accuracy without sacrificing computational time. This is because computing a function is faster and more advantageous than iteratively summing a series.

4 PROPOSED GUIDANCE LAWS

This section presents ITCG laws to achieve interception at the desired impact time while preserving the characteristics of PPNG. The guidance laws follow BPNG structure consisting of the PPNG as the baseline guidance and the bias input for the regulation of impact time error. The

guidance command can be represented as

$$a_m = a_{PPN} + a_{bias} = -N\frac{V_m^2}{r}\sin\sigma + a_{bias} \tag{24}$$

where a_{bias} is the biased term to be designed. Substitution of Eq. (24) into Eq. (3) yields the differential equation of σ as

$$\dot{\sigma} = -(N-1)\frac{V_m}{r}\sin\sigma + \frac{a_{bias}}{V_m} \tag{25}$$

Note that it is possible to design a_{bias} in various ways for the impact-time-control. In this study, two approaches for bias input design are proposed based on the exact time-to-go of the baseline trajectory. In Sec. 4.1, a time-to-go error feedback law is designed using the exact time-to-go solution of the PPNG. In Sec. 4.2, a look-angle control guidance law is proposed for impact-time-control considering the look angle constraint. The characteristics of the proposed guidance laws are discussed in Sec. 4.3.

4.1 Guidance Law 1: Direct impact-time-control Based on Exact Time-to-Go

In this section, an ITCG law is designed using the explicit feedback of impact time error. Let us define the time-to-go error as

$$e_t = t_{go,PPN} - t_{go}^d \tag{26}$$

where $t_{go}^d = t_d - t$ is the desired time-to-go.

The desired time-to-go should be chosen within the feasible region, otherwise the guidance objectives cannot be achieved simultaneously. Considering the physical constraints, one may select the feasible region $\Gamma \in (\frac{r}{V_m}, \frac{r}{V_m\cos\sigma_{\lim}})$ for the desired time-to-go (Lee et al. 2020).

First, let us design the bias input for stabilizing the error variable defined in Eq. (26). For this, taking the time derivative of e_t along the closed-loop trajectory by the guidance command, Eq.

(24), and substituting Eqs. (2), (18)-(20), and (25), into the resulting equation yields

$$\begin{aligned}\dot{e}_t &= \dot{t}_{go,PPN} - (-1) = \frac{\partial t_{go,PPN}}{\partial r}\dot{r} + \frac{\partial t_{go,PPN}}{\partial |\sigma|}\dot{\sigma} sgn(\sigma) + 1 \\ &= \frac{t_{go,PPN}}{r}\left(-V_m \cos\sigma\right) + 1 + \frac{1}{N-1}\frac{t_{go,DPP} - t_{go,PPN}}{\tan|\sigma|}\left(-(N-1)\frac{V_m}{r}\sin\sigma + \frac{a_{bias}}{V_m}\right) sgn(\sigma) \\ &= \frac{1}{(N-1)V_m}\frac{t_{go,DPP} - t_{go,PPN}}{\tan\sigma} a_{bias} \\ &\triangleq B_t(\sigma) a_{bias}\end{aligned} \tag{27}$$

where $sgn(x)$ is defined as

$$sgn(x) = \begin{cases} 1 & x > 0 \\ 0 & x = 0 \\ -1 & x < 0 \end{cases} \tag{28}$$

The error dynamics of Eq. (27) are linear in a_{bias}. According to Eqs. (19) and (21), if the absolute value of the look angle is bounded as $|\sigma| > \underline{\sigma} > 0$, then B_t is also bounded as

$$|B_t(\sigma)| \geq \frac{1}{V_m}\left.\frac{\partial t_{go,PPN}}{\partial \sigma}\right|_{\sigma=\underline{\sigma}} > 0 \tag{29}$$

The bias input should be properly designed to stabilize the error dynamics while satisfying the look angle constraint. For this, let us propose the bias input a_{bias} as

$$a_{bias,1} = -(N-1)\frac{V_m^2}{r}\sin\sigma_{\lim}\left(sgn(\sigma) f(\sigma)\right) sgn(e_t)\left(\frac{|e_t|}{|e_t(0)|}\right)^{\alpha} \tag{30}$$

where $0 < \alpha \leq 1$ is a positive parameter introduced for finite-time convergence.

Note that $\alpha = 1$ represents the linear error feedback with state-dependent varying gain and $f(\sigma)$ is a smooth shaping function satisfying the following conditions (Kim et al. 2019b; Kim et al. 2021)

$$\begin{aligned} f(\sigma) &\geq 1 \quad \text{if} \quad \sigma \in \Sigma \\ f(\sigma) &= 1 \quad \text{if} \quad \sigma = \pm\sigma_{\lim} \end{aligned} \tag{31}$$

The shaping function is required for preserving the positive invariance of the set Σ. One may choose the shaping function from various functions satisfying the boundary conditions. The error dynamics associated with the bias input $a_{bias,1}$ can be expressed by using Eq. (30) in Eq. (27) as

$$\begin{aligned}\dot{e}_t &= B_t(\sigma)a_{bias,1} = \frac{1}{(N-1)V_m}\frac{t_{go,DPP}-t_{go,PPN}}{\tan\sigma}a_{bias,1}\\ &= -V_m\sin\sigma_{\lim}\left(\frac{t_{go,DPP}-t_{go,PPN}}{\tan\sigma}\right)\frac{1}{r}\frac{\sigma}{|\sigma|}f(\sigma)sgn(e_t)\left(\frac{|e_t|}{|e_t(0)|}\right)^{\alpha}\\ &= -V_m\sin\sigma_{\lim}\left(\frac{t_{go,DPP}-t_{go,PPN}}{|\tan\sigma|}\right)\frac{1}{r}f(\sigma)sgn(e_t)\left(\frac{|e_t|}{|e_t(0)|}\right)^{\alpha}\end{aligned} \tag{32}$$

For stability analysis, let us consider the following Lyapunov candidate function.

$$V_1 = \frac{1}{2}e_t^2 \tag{33}$$

The time derivative of V_1 along the error dynamics given by Eq. (32) can be obtained substituting Eq. (19) as

$$\begin{aligned}\dot{V}_1 &= \dot{e}_t e_t = -V_m\sin\sigma_{\lim}\left(\frac{t_{go,DPP}-t_{go,PPN}}{|\tan\sigma|}\right)\frac{f(\sigma)}{r}\frac{|e_t|^{1+\alpha}}{|e_t(0)|^{\alpha}}\\ &= -(N-1)V_m\sin\sigma_{\lim}\left(\frac{\partial t_{go,PPN}}{\partial|\sigma|}\right)\frac{f(\sigma)}{r}\frac{(2V_1)^{\frac{1+\alpha}{2}}}{|e_t(0)|^{\alpha}} \le 0\end{aligned} \tag{34}$$

Note that $N > 2$. According to Eq. (21), V_1 monotonically decreases as long as $\sigma \neq 0$. To demonstrate the finite-time convergence of the error e_t, the Lyapunov function is further expanded by using Eqs. (2), (9), (12), (17) (19), (20) and (30) into Eq. (34) as

$$\begin{aligned}\dot{V}_1 &= (N-1)\sin\sigma_{\lim}\left(\frac{\partial t_{go,PPN}}{\partial|\sigma|}\right)\frac{-V_m\cos\sigma}{r}\frac{f(\sigma)}{\cos\sigma}\frac{(2V_1)^{\frac{1+\alpha}{2}}}{|e_t(0)|^{\alpha}}\\ &= (N-1)\sin\sigma_{\lim}\left(\frac{\partial t_{go,PPN}}{\partial|\sigma|}\right)\frac{\dot{r}}{r}\frac{f(\sigma)}{\cos\sigma}\frac{(2V_1)^{\frac{1+\alpha}{2}}}{|e_t(0)|^{\alpha}}\\ &\le \frac{2^{\frac{1+\alpha}{2}}\sin\sigma_{\lim}}{|e_t(0)|^{\alpha}}V_1^{\frac{1+\alpha}{2}}\left(\frac{t_{go,DPP}-t_{go,PPN}}{|\tan\sigma|}\right)\frac{\dot{r}}{r} = \frac{2^{\frac{1+\alpha}{2}}\sin\sigma_{\lim}}{V_m|e_t(0)|^{\alpha}}V_1^{\frac{1+\alpha}{2}}\left(\frac{\sec\sigma-\mathcal{F}(|\sigma|;N)}{|\tan\sigma|}\right)\dot{r}\\ &= \frac{2^{\frac{1+\alpha}{2}}(N-1)\sin\sigma_{\lim}}{V_m|e_t(0)|^{\alpha}}V_1^{\frac{1+\alpha}{2}}\left(\frac{\partial\mathcal{F}(|\sigma|;N)}{\partial|\sigma|}\right)\dot{r}\end{aligned} \tag{35}$$

It is desired to regulate the time-to-go error before $(r,\sigma)\to(0,0)$ to recover the performance of

the baseline guidance. Let $r_1 > 0$ be a required distance at which the time-to-go error vanishes, and σ_1 is the corresponding look angle. The stability of the time-to-go error dynamics leads to $\sigma \in [\underline{\sigma}, \bar{\sigma}] \subset \Sigma/\{0\}$ and $\frac{\partial \mathcal{F}}{\partial \sigma}\big|_{\underline{\sigma}} \leq \frac{\partial \mathcal{F}}{\partial \sigma}$. Equation (35) can be rewritten as

$$\frac{dV_1}{V_1^{\left(\frac{1+\alpha}{2}\right)}} \leq C_1 dr \tag{36}$$

where $C_1 = \frac{2^{\frac{1+\alpha}{2}}(N-1)\sin\sigma_{\lim}}{V_m |e_t(0)|^{\alpha}} \frac{\partial \mathcal{F}}{\partial \sigma}\big|_{\underline{\sigma}}$.

Integrating both sides of Eq. (36) gives

$$\frac{2}{1-\alpha}\left((V_1(r))^{\left(\frac{1-\alpha}{2}\right)} - (V_1(0))^{\left(\frac{1-\alpha}{2}\right)}\right) \leq C_1 (r - r_0) \tag{37}$$

Considering the boundary condition $V_1(r_1) = 0$, the settling distance r_1 is bounded from below as described by

$$r_1 \geq r_{1,\min} = r_0 - \frac{2}{C_1 (1-\alpha)} V_1(0)^{\frac{1-\alpha}{2}} = r_0 - \frac{V_m}{(N-1)(1-\alpha)\sin\sigma_{\lim} \frac{\partial \mathcal{F}}{\partial \sigma}\big|_{\underline{\sigma}}} |e_t(0)| \tag{38}$$

From Eq. (38), smaller α and $|e_t(0)|$ result in larger $r_{1,\min}$, contributing to faster time-to-go error convergence.

Considering the seeker's FOV limit, the proposed guidance law should ensure the positive invariance of Σ. To investigate this property, let us rewrite the σ-dynamics as

$$\dot{\sigma} = -(N-1)\frac{V_m}{r}\left(\sin\sigma + \sin\sigma_{\lim} f(\sigma) \frac{\sigma}{|\sigma|} sgn(e_t) \left(\frac{|e_t|}{|e_t(0)|}\right)^{\alpha}\right) \tag{39}$$

Consider the storage function V_σ defined as

$$V_\sigma(\sigma) = \frac{1}{2}(\sin\sigma)^2 \tag{40}$$

Note that the set $M = \left\{\sigma(t) : V_\sigma(|\sigma(t)|) \leq V_\sigma(\sigma_{\lim}), \quad \forall t \in [t_0, t_f]\right\}$ is equivalent to Σ. Therefore,

using the Lyapunov stability theory, the positively invariant set Σ can be proved by showing that the M is a positively invariant level set. By differentiating Eq. (40) with respect to time, and using Eq. (39) in the resulting equation, we obtain the time derivative of the storage function evaluated at the boundary as

$$\dot{V}_\sigma(\pm\sigma_{\lim}) = -(N-1)\frac{V_m}{r}\cos\sigma_{\lim}\sin^2\sigma_{\lim}\left(1 + f(\sigma_{\lim})sgn(e_t)\left(\frac{|e_t|}{|e_t(0)|}\right)^\alpha\right) < 0 \tag{41}$$

Note that the terms inside the bracket of Eq. (41) is greater than zero because of the boundary condition of $f(\sigma_{\lim}) = 1$. Therefore, M is a positively invariant set, and so is Σ.

4.2 Guidance Law 2: Indirect impact-time-control via Look-Angle Control

This section presents an indirect approach to design an ITCG by controlling the look angle (Kim et al. 2021). Suppose that the desired impact time is achieved by the baseline guidance law, i.e., PPNG. Then, the desired look angle associated with the desired impact time can be determined by

$$t_{go}^d = t_{go,PPN}^d\left(r, |\sigma_d|; N\right) = \frac{r}{V_m}\mathcal{F}\left(|\sigma_d|; N\right) \tag{42}$$

There exists a one-to-one correspondence between $|\sigma|$ and $t_{go,PPN}$, and therefore the desired value $|\sigma_d|$ can be obtained by the inverse mapping of Eq. (42) as

$$|\sigma_d| = \mathcal{F}^{-1}\left(\frac{V_m}{r}t_{go,PPN}^d; N\right) \tag{43}$$

Note that the inverse mapping cannot be analytically obtained because the inverse of the GHGF $\mathcal{F}(|\sigma|; N)$ is not available. Since $\mathcal{F}(|\sigma|; N)$ is monotonically increasing on the interval $|\sigma| \in [0, \sigma_{\lim}]$, $|\sigma_d|$ can be easily obtained by numerical methods developed for line search or root finding. To resolve the sign ambiguity of σ, σ_d can be determined using the current sign of the current look angle as follows:

$$\sigma_d = |\sigma_d| sgn(\sigma) \tag{44}$$

The desired look angle σ_d varies with elapsed time. The time derivative can be obtained by

differentiating Eq. (42) with respect to time and using Eqs. (2), (17)-(19) in the resulting equation as

$$-1 = \frac{\partial t_{go,PPN}}{\partial r}\dot{r} + \frac{\partial t_{go,PPN}}{\partial |\sigma_d|}\dot{\sigma}_d sgn(\sigma_d) = \frac{t_{go,PPN}}{r}\left(-V_m \cos\sigma\right) + \frac{\cot\sigma_d}{N-1}\left(t_{go,DPP} - t_{go,PPN}\right)\dot{\sigma}_d \tag{45}$$

where $t_{go,PPN}$ and $t_{go,DPP}$ in Eq. (45) are the values obtained from the desired look angle σ_d.

Using Eqs. (12) and (19), Eq. (45) can be rewritten with respect to $\dot{\sigma}_d$ as

$$\begin{aligned}\dot{\sigma}_d &= -(N-1)\frac{V_m}{r}\left(\frac{r}{V_m} - \cos\sigma\, t_{go,PPN}\right)\frac{\tan\sigma_d}{t_{go,DPP} - t_{go,PPN}} \\ &= -(N-1)\frac{V_m}{r}\frac{1-\cos\sigma\mathcal{F}\left(\sigma_d;N\right)}{1-\cos\sigma_d\mathcal{F}\left(\sigma_d;N\right)}\sin\sigma_d\end{aligned} \tag{46}$$

where $\mathcal{F}\left(\sigma_d;N\right)$ can be calculated from Eq. (13).

Note that there is a symmetric relation between the time-to-go and the look angle, and the look angle is within the symmetric bound, i.e., $-\sigma_{\lim} \le \sigma \le \sigma_{\lim}$. Without a loss of generality, let us consider the positive look angle case $\sigma > 0$ and $\sigma_d > 0$.

For guidance law design, let us define the error variable e_σ for the impact-time-control as

$$e_\sigma = \sigma - \sigma_d \tag{47}$$

Taking time derivative of Eq. (47) and using Eqs. (25) and (46) in the resultant equation, the error dynamics of e_σ can be obtained as

$$\begin{aligned}\dot{e}_\sigma &= -(N-1)\frac{V_m}{r}\sin\sigma + (N-1)\frac{V_m}{r}\frac{1-\cos\sigma\mathcal{F}\left(\sigma_d;N\right)}{1-\cos\sigma_d\mathcal{F}\left(\sigma_d;N\right)}\sin\sigma_d + \frac{a_{bias}}{V_m} \\ &\triangleq \left(F_\sigma\left(\sigma,r\right) - \dot{\sigma}_d\left(\sigma,\sigma_d,r\right)\right) + \frac{1}{V_m}a_{bias}\end{aligned} \tag{48}$$

where

$$F_\sigma(\sigma,r) = -(N-1)\frac{V_m}{r}\sin\sigma \tag{49}$$

Considering the guidance objectives stated in Sec. 2.2, the look angle σ should remain in Σ for

all time. For this, let us propose the bias input as

$$a_{bias,2} = -V_m \left(F_\sigma(\sigma, r) - \dot{\sigma}_d\right) - (N-1)\frac{V_m^2}{r}\cos\sigma \left(k f(\sigma)\right) sgn(e_\sigma) \left(\frac{|e_\sigma|}{|e_\sigma(0)|}\right)^\alpha \tag{50}$$

where $k > 0$ is a design parameter, and $f(\sigma)$ is the shaping function defined as same as in Sec. 4.1.

The first term of $a_{bias,2}$ cancels out the nonlinear effect of the error dynamics, and the second term is a feedback term to achieve the finite-time convergence of e_σ as well as the positive invariance of Σ. The error dynamics of e_σ associated with the biased input can be expressed as

$$\dot{e}_\sigma = -(N-1)\frac{V_m}{r}\cos\sigma k f(\sigma) sgn(e_\sigma) \left(\frac{|e_\sigma|}{|e_\sigma(0)|}\right)^\alpha \tag{51}$$

To verify the stability of the proposed guidance law, let us introduce the following Lyapunov candidate function.

$$V_2 = \frac{1}{2}e_\sigma^2 \tag{52}$$

Differentiating Eq. (52) with respect to time, and substituting Eq. (50) into the resulting equation yields the time derivative of V_2 along the error dynamics of e_σ as

$$\dot{V}_2 = -(N-1)\frac{V_m \cos\sigma}{r} k f(\sigma) \frac{|e_\sigma|^{1+\alpha}}{|e_\sigma(0)|^\alpha} < 0 \tag{53}$$

Equation (53) shows that $\dot{V}_2$ is negative definite becomes $N > 2$ and $f(\sigma) \geq 1$, and therefore the equilibrium point $e_\sigma = 0$ is asymptotically stable.

Now, let us demonstrate the finite-time convergence of the error variable. Substituting Eqs. (2), (52), and the condition $f(\sigma) \geq 1$ into Eq. (53) gives

$$\frac{\dot{V}_2}{V_2^{\frac{1+\alpha}{2}}} \leq (N-1)\frac{2^{\frac{1+\alpha}{2}}}{|e_\sigma(0)|^\alpha}\frac{\dot{r}}{r}k \tag{54}$$

$$V_2^{-\frac{1+\alpha}{2}} dV_2 \leq C_2 k \frac{1}{r} dr \tag{55}$$

where $C_2 = (N-1)\frac{2^{\frac{1+\alpha}{2}}}{|e_\sigma(0)|^\alpha}$.

Integrating each side of Eq. (55) gives

$$\frac{2}{1-\alpha}\left(V_2(r)^{\frac{1-\alpha}{2}} - V_2(r_0)^{\frac{1-\alpha}{2}}\right) \leq kC_2 \ln\left(\frac{r}{r_0}\right) \tag{56}$$

Considering the boundary condition for the finite-time convergence, i.e., $V_2(r) = 0$, $r \geq r_{s2}$, the settling distance r_{s2} can be bounded from below as

$$\begin{aligned} r_{s2} \geq r_{s2,\min} &:= r_0 \exp\left(\frac{-2}{(1-\alpha)k(N-1)\frac{2^{\frac{1+\alpha}{2}}}{|e_\sigma(0)|^\alpha}} V_2(r_0)^{\frac{1-\alpha}{2}}\right) \\ &= r_0 \exp\left(-\frac{|e_\sigma(0)|}{(1-\alpha)k(N-1)}\right) \end{aligned} \tag{57}$$

During the maneuver, σ should be kept consistently in Σ. If the desired value is consistently in the invariant set Σ, convergence of e_σ to zero along the dynamics of Eq. (51) automatically ensures the positive invariance of Σ. That is, $\sigma_d \in \Sigma\, \forall t \in [t_0, t_f] \Rightarrow \sigma \in \Sigma$ as $\sigma \to \sigma_d$. In this respect, let us consider the case that the desired look angle is initially set beyond the limited value, i.e., $\sigma_{d0} > \sigma_{\lim}$. Then, the time derivative of the look angle satisfies

$$\begin{aligned} \dot{\sigma}_d(\sigma, \sigma_d, r)\,\sigma = -(N-1)\frac{V_m}{r}\left(\frac{1-\cos\sigma\mathcal{F}(\sigma_d; N)}{1-\cos\sigma_d\mathcal{F}(\sigma_d; N)}\right)\sin\sigma_d\sigma < 0 \\ \text{if} \quad \cos^{-1}\left(\frac{1}{\mathcal{F}(\sigma_d; N)}\right) \leq |\sigma| \leq \sigma_{\lim} \end{aligned} \tag{58}$$

Figure 2 shows the typical profiles of the desired look angle. If the initial look angle satisfies $\sigma_0 < \cos^{-1}\left(\frac{1}{\mathcal{F}(\sigma_{d0};N)}\right) < \sigma_{\lim} < \sigma_{d0}$, the desired look angle increases with increasing look angle to regulate the error. Then, the desired look angle reaches the maximum value at which the desired value σ_d^* and the instant look angle σ^* satisfy $\mathcal{F}(\sigma_d^*; N) = \frac{1}{\cos\sigma^*}$. Then, the desired look angle monotonically decreases, $\sigma_d^* > \sigma_d$. On the other hand, if the initial look angle and the desired

value initially satisfy $\cos^{-1}\left(\frac{1}{\mathcal{F}(\sigma_{d0};N)}\right) < \sigma_0 < \sigma_{\lim} < \sigma_{d0}$, then the desired value monotonically decreases from the initial phase. To ensure the error regulation while maintaining the look angle constraint, the guidance gain k should be properly determined. From Eqs. (45), (46) and (50), the time derivative of σ at the boundary can be expressed as

$$\begin{aligned}\dot{\sigma}|_{\sigma=\sigma_{\lim}} &= \dot{\sigma}_d - (N-1)\frac{V_m}{r}\cos\sigma_{\lim} k f(\sigma_{\lim}) sgn(e_\sigma)\left(\frac{|e_\sigma|}{|e_\sigma(0)|}\right)^\alpha \\ &= -(N-1)\frac{V_m}{r}\left(\left(\frac{1-\cos\sigma_{\lim}\mathcal{F}(\sigma_d;N)}{1-\cos\sigma_d\mathcal{F}(\sigma_d;N)}\right)\sin\sigma_d + \cos\sigma_{\lim} k f(\sigma) sgn(e_\sigma)\left(\frac{|e_\sigma|}{|e_\sigma(0)|}\right)^\alpha\right)\end{aligned} \tag{59}$$

Note that $f(\sigma_{\lim}) = 1$. For the storage function V_σ defined in Eq. (40), $\dot{V}_\sigma$ at the boundary $\sigma = \sigma_{\lim}$ can be obtained as

$$\begin{aligned}\dot{V}_\sigma(\sigma_{\lim}) = \cos\sigma_{\lim}\sin\sigma_{\lim}\dot{\sigma}|_{\sigma=\sigma_{\lim}} = -(N-1)\frac{V_m}{r}\cos\sigma_{\lim}\sin\sigma_{\lim} \\ \left(\frac{1-\cos\sigma_{\lim}\mathcal{F}(\sigma_d;N)}{1-\cos\sigma_d\mathcal{F}(\sigma_d;N)}\sin\sigma_d + \cos\sigma_{\lim} k sgn(e_\sigma)\left(\frac{|e_\sigma|}{|e_\sigma(0)|}\right)^\alpha\right)\end{aligned} \tag{60}$$

At the boundary $\sigma = \sigma_{\lim}$, the following inequalities hold

$$1 > \frac{1-\cos\sigma_{\lim}\mathcal{F}(\sigma_d;N)}{1-\cos\sigma_d\mathcal{F}(\sigma_d;N)} \geq \frac{1-\cos\sigma_{\lim}\mathcal{F}\left(\sigma_d^*;N\right)}{1-\cos\sigma_d^*\mathcal{F}\left(\sigma_d^*;N\right)} =: \underline{\Delta} > 0 \tag{61a}$$

$$\sin\sigma_d\sin\sigma_{\lim} > \sin^2\sigma_{\lim} \tag{61b}$$

Using the above inequalities, the upper bound of the design parameter can be determined as

$$k < \tan\sigma_{\lim}\underline{\Delta} \tag{62}$$

Then, $\dot{V}_\sigma$ is bounded above zero as

$$\dot{V}_\sigma(\sigma_{\lim}) \leq -(N-1)\frac{V_m}{r}\cos\sigma_{\lim}\underline{\Delta}\sin^2\sigma_{\lim}\left(1 + \frac{k}{\underline{\Delta}\tan\sigma_{\lim}} sgn(e_\sigma)\left(\frac{|e_\sigma|}{|e_\sigma(0)|}\right)^\alpha\right) < 0 \tag{63}$$

In summary, the design parameter k should be bounded by $0 < k \leq \tan\sigma_{\lim}\underline{\Delta}$. The lower

bound is made for error tracking, and the upper bound ensures that the look angle will not to exceed the FOV limit while tracking the desired look angle, respectively.

Remark 3. (Prevention of singularity of biased command when $t_{go} \in \left(\frac{r}{V_m}, t_{go,PPN}\right)$) The desired time-to-go can be smaller than the predicted time-to-go for the PPNG. In that case, it should be guaranteed that the lead angle profile does not maintain zero in a finite interval. One way to avoid the singularity is to reset the navigation gain N depending on the desired impact time. If the impact time is smaller than the PPNG for the current gain set, $t_{go}^d < t_{go,PPN}$, then N can be increased to reduce the current t_{go} so that $t_{go,PPN}(N_{new}) < t_{go}^d$. Afterwards, the biased term will contribute to elongating the flight path in order to achieve the desired impact time.

4.3 Discussions of Proposed Guidance Laws

Behaviors of Guidance Laws and Guidelines for Design Parameter Selection

In this section, let us discuss how the proposed guidance laws behave from the perspective of BPNG. In the initial period of the terminal phase, two guidance components, a_{PPNG} and a_{bias} consistently steer the missile heading to enter a collision course for desired impact time. In this period, the effect of the bias input is dominant in the guidance command. The time-to-go error indicates the predicted intercept time error when the baseline guidance is only in action. The correction of the impact time error implies that the initial condition is being adjusted to the proper one to finish the PPNG at the desired impact time. Once the error dynamics are stabilized, then the guidance command becomes equivalent to PPNG. The time-to-go is obtained based on the PPNG, and therefore the error correction can be performed by complying with the performance of the baseline guidance. As a whole, the stabilization of the error dynamics plays the most important role in this framework. This study employs the finite-time convergent error dynamics that appear in many pieces of literature on sliding mode control scheme (Shtessel et al. 2007; Levant 2001; Zhang et al. 2014). Three kinds of design parameters contribute to stabilizing the error dynamics. The properties of the parameters on the performance of the guidance laws are discussed as follows.

- (Exponent of the error, α) : α attributes to the nonlinear error feedback and leads to finite-

time convergence of the error dynamics. The lower α improves the convergent rate of the error dynamics but rapidly drives the error to be regulated and causes a non-uniform response when the error is close to zero. To prevent this issue, it is recommended to choose α carefully and properly.

- (Shaping function, $f(\sigma)$) : $f(\sigma)$ generally acts as the varying gain in terms of σ that shapes the trajectory, which also ensures that the look angle remains within the limit value. Considering the boundary condition (31), one may choose an even and concave function with different basis. For example, if the smooth "hat-shaped" function is considered, which is mostly flat over the interval $\sigma \in (-\sigma_{\text{lim}} + \epsilon, \sigma_{\text{lim}} - \epsilon)$ for a small constant ϵ and changes to 1 rapidly at $\sigma = \pm\sigma_{\text{lim}}$, then the maneuver abruptly changes to keep look angle within the limit value. As the extreme case, $\epsilon \to 0$, the shaping function is made a discontinuous form, and the response becomes similar to two-stage guidance approach (Sang and Tahk 2009; Tekin et al. 2017a; Lee et al. 2020). This maneuver may take advantages of the look angle keeping and yield a large achievable impact time set (Tekin et al. 2017a; Lee et al. 2020) but also brings an abrupt guidance command.
- (Proportional Feedback in the second approach, k) : k mainly amplifies the effect of the error terms in the bias input. A large k increases the convergent rate of the error response, but it should be bounded by Eq. (62) for the consideration of look angle limit. One possible way to select k is to consider the linearized formulation as Eq. (68).

Comparison with Inaccurate Time-to-go

This section examines how the exact solution improves the impact time control compared to the approximate one. Aforementioned in Remark 1, the impact time error e_t can be expressed in terms of the approximate solution as

$$e_t = t_{go,PPN} - t_{go}^d = t_{go,approx} + \Delta_t - t_{go}^d = e_{t,approx} + \Delta_t \tag{64}$$

where Δ_t is the time-to-go between the exact solution and the approximate one. Note that Δ_t consists of higher-order terms expressed as r and σ, which vary with respect to time. For brevity, it is assumed that $|\Delta_t| \leq b_1$ and $|\dot{\Delta}_t| \leq b_2$ for small positive b_1 and b_2. Suppose that guidance laws based on the approximate time-to-go solution are properly designed so that the closed-loop dynamics become Hurwitz as $\dot{e}_{t,approx} = -K_1 e_{t,approx}$. Then, the true error dynamics e_t can be obtained as

$$\dot{e}_t = -K_1 e_{t,approx} + K_1 \Delta_t + \dot{\Delta}_t \tag{65}$$

Therefore, the residual error $\Delta \triangleq K_1 \Delta_t + \dot{\Delta}_t$ prevents the error from converging to zero unless it is suppressed. Note also that even the small impact time error induces the fast diverging response to the LOS rate and causes large miss distance. On the other hand, the proposed guidance laws utilize the exact time-to-go and fully account for the true impact time error. Therefore, the residual error is compensated, which improves the impact time precision and decreases the miss distance.

Comparison Between Proposed Guidance Laws

The proposed guidance laws using both approaches comply with BPNG structure and exhibit common characteristics discussed in Sec. 4.3. This section addresses the comparison between the proposed guidance laws in regard to similarities and distinct properties. First, let us examine the differences in the commands. The main differences between the guidance laws presented in Secs. 4.1 and 4.2 are as follows: i) controlled variables (e_t, e_σ), and ii) design parameters ($f(\sigma)$, k). Let us consider an approximate time-to-go under the small angle assumption, Eq. (23). Assuming that σ_d is obtained from the approximate solution, the impact time error can be approximated using the Taylor series expansion as

$$\begin{aligned} e_t \approx \hat{t}_{go,PPN} - \hat{t}^d_{go,PPN} &= \frac{r}{V_m}\left(1 + \frac{\sigma^2}{2(2N-1)}\right) - \frac{r}{V_m}\left(1 + \frac{\sigma_d^2}{2(2N-1)}\right) \\ &= \frac{r}{2(2N-1)V_m}\left(\sigma^2 - \sigma_d^2\right) \end{aligned} \tag{66}$$

The bias input $a_{bias,1}$ in the guidance law 1, Eq. (30), for $\alpha = 1$ can be rewritten as

$$\begin{aligned} a_{bias,1} &= -(N-1)V_m^2 \frac{\sin\sigma_{\lim}}{r}\left[sgn(\sigma)f(\sigma)\right]\left(\frac{e_t}{|e_t(0)|}\right) \\ &\approx -(N-1)V_m^2 \frac{\sin\sigma_{\lim}}{r_0}\left[sgn(\sigma)f(\sigma)\right]\frac{\sigma^2-\sigma_d^2}{|\sigma_0^2-\sigma_{d,0}^2|} \end{aligned} \tag{67}$$

Considering Eq. (67), the design parameter k can be chosen to express the guidance law 2, Eq. (50), in a form similar to the guidance law 1. The particular k can be chosen as

$$k = sgn(\sigma)\frac{\sigma+\sigma_d}{|\sigma_0+\sigma_{d,0}|}\frac{r}{r_0}(\tan\sigma_{\lim})\,\underline{\Delta} \le \tan\sigma_{\lim}\,\underline{\Delta} \tag{68}$$

Setting $\alpha = 1$, the bias input $a_{bias,2}$ in the guidance law 2 can be rewritten as

$$\begin{aligned} a_{bias,2} &= -V_m\left(F_\sigma(\sigma,r)-\dot{\sigma}_d\right) - (N-1)\frac{V_m^2}{r_0}\sin\sigma_{\lim} sgn(\sigma)\left(\frac{\cos\sigma}{\cos\sigma_{\lim}}\right)\underline{\Delta}\, f(\sigma)\frac{\sigma^2-\sigma_d^2}{|\sigma_0^2-\sigma_{d,0}^2|} \\ &= -V_m\left(F_\sigma(\sigma,r)-\dot{\sigma}_d\right) + \frac{\cos\sigma}{\cos\sigma_{\lim}}\underline{\Delta}\, a_{bias,1} \end{aligned} \tag{69}$$

It can be observed from the approximated guidance laws that their similarities arise from the feedback action. In the guidance law 2, $a_{bias,2}$, the feedback part is roughly proportional to $a_{bias,1}$, but $a_{bias,2}$ also contains nonlinear cancellation terms, as shown in Eq. (69). The feedback action is reduced as the look angle approaches the limited value.

$$\frac{\cos\sigma}{\cos\sigma_{\lim}}\underline{\Delta}|a_{bias,1}| \approx \underline{\Delta}|a_{bias,1}| << |a_{bias,1}|, \quad \text{as} \quad \sigma \to \sigma_{\lim} \tag{70}$$

Meanwhile, one can also differentiate the proposed guidance laws using two approaches from one another. In the first approach, the guidance law utilizes the impact time error based on exact time-to-go. In this aspect, it can be regarded that the direct control of the impact time error is a more intuitive way to deal with the impact time control. The guidance law could also be much robust if the measurement error is involved in practice. On the other hand, in the second approach, the reference profile can be modified for trajectory shaping in addition to selecting design parameters.

As shown in Fig. 2, the look angle constraint can be incorporated into the design of the look angle reference. The look angle reference σ_r can be defined not to exceed the FOV limit as described by

$$\sigma_r = sgn(\sigma_d) \min\left(|\sigma_d|, \sigma_{\lim}\right) \tag{71}$$

The guidance law considering the reference profile can be designed to regulate the look angle error between σ and σ_r as

$$a_{bias,2a} = -V_m \left(\left(F_\sigma\left(\sigma_r, r\right) - \varphi(e_\sigma, \sigma)\dot{\sigma}_d\right) + K(r,\sigma)\frac{\sigma - \sigma_r}{|e_\sigma(0)|} \right) \tag{72}$$

where $K(r,\sigma) > 0$ is the positive gain function for a feedback action. In Eq. (72), $\varphi(e_\sigma, \sigma)$ is an activation function defined as follows

$$\varphi(e_\sigma, \sigma) = \begin{cases} 1 & \text{if} \quad \dot{\sigma}_d e_\sigma < 0 \\ 0 & \text{if} \quad \dot{\sigma}_d e_\sigma \geq 0 \end{cases} \tag{73}$$

Note that the desired look angle σ_d is replaced by σ_r in Eq. (72). Through these processes, the similarity between the reference tracking law and two-stage guidance laws (Lee et al. 2020) can be shown. Assume that the look angle reference is generated considering the limit value $\sigma_0 \leq \sigma_{\lim} < \sigma_d$. Then, the bias reference allows the look angle to follow the limit value. After the look angle converges to the reference $\sigma_r = \pm\sigma_{\lim}$ at the instant t_1, the trajectory by the proposed guidance law is equivalent to that presented in (Lee et al. 2020). After σ converges to σ_r, the profile of σ can be obtained as (Lee et al. 2020)

$$\sigma(t) = \begin{cases} \sigma_{\lim}, & r_{sw} \leq r \leq r_1 \\ \sin^{-1}\left(\sin\sigma_{\lim}\left(\frac{r}{r_{sw}}\right)^{N-1}\right), & 0 \leq r \leq r_{sw} \end{cases} \tag{74}$$

where r_{sw} is the transition range that can be calculated as

$$r_{sw} = V_m \frac{\frac{r_1}{V_m \cos\sigma_{\lim}} - (t^d - t_1)}{\sec\sigma_{\lim} - \mathcal{F}(\sigma_{\lim}; N)} \tag{75}$$

The maintaining the limit value continues until σ_r changes to σ_d. After σ_r transition, the look angle error is regulated. Then, the resultant guidance law is governed by the PPNG. In this fashion, the second approach using the reference, $a_{bias,2a}$, would produce wider set of the achievable impact time than the first approach. In comparison to the two-stage guidance law (Lee et al. 2020), the feedback action of the proposed method makes the guidance system more robust against the initial heading error and model uncertainty.

5 NUMERICAL SIMULATION

Numerical simulations were conducted to evaluate the performance of the proposed guidance laws in three different scenarios. In all simulation cases, the initial distance between the missile and target was set to $10,000$ m, the missile speed was set to 300 m/s, and the initial look angle was 30°. The missile's maximum acceleration was set to 300 m/s^2, and the FOV limit was set to 60°. A navigation constant of $N = 3$ was chosen, and the simulation step size was set to 500 Hz. Other parameters were scenario-dependent. The simulations were terminated when the relative distance r between the missile and target was less than 0.3.

5.1 Scenario 1: Performance Effects of Design Parameters

In the first scenario, the bias input $a_{bias,1}$ is considered among the three proposed guidance laws, and the effect of the design parameters $f(\sigma)$ and α on the performance of the proposed guidance law 1 is investigated. As discussed in Sec. 4.3, the shaping function $f(\sigma)$ and the exponent α will affect the performance, and the following shaping functions are considered.

$$f_1(\sigma) = \left(\frac{\cos\sigma}{\cos\sigma_{\lim}}\right)^p, \quad f_2(\sigma) = 1 + a\left(1 - \left(\frac{|\sigma|}{\sigma_{\lim}}\right)^b\right) \tag{76}$$

where $(p, a, b) = (6, 63, 5)$ are chosen. Table 1 summarizes the simulation cases considered in this scenario.

Figure 3 shows the simulation results of the first scenario. To achieve the desired impact time, the missile steers to increase the look angle. As the look angle approaches the FOV limit, the guidance law enables the look angle not to exceed the FOV limit. As shown in Fig. 3e, the smooth and continuous response is observed in the guidance command while achieving the look angle constraint and impact time, which is advantageous over multi-stage type guidance laws (Lee et al. 2020). The shaping function exerts substantial influences on the performance as it adjusts the trend of the trajectory. In comparison to the case using f_1, the look angle approaches closer to the boundary and stays near the boundary for a longer period of time when f_2 is used. As shown in Fig. 3d, the graph of the function f_2 is flat around the origin and changes sharply near the FOV limit. The flattened shaping function creates a tendency for the look angle to be maintained near the look angle boundary. Meanwhile, it is observed that a smaller α reduces regulation time as shown in Fig. 3c. It can be concluded that the shaping function mainly affects the initial phase of the flight while the exponent α influences the regulation time. It is also found that the performance is sensitive to the change of α when f_1 is used as the shaping function, which indicates that the design parameters should be selected in pairs.

5.2 Scenario 2: Comparison with Guidance Laws Based on Approximate Time-to-Go

In the second scenario, the effect of the time-to-go accuracy on the ITCG is evaluated. The missile is required to intercept the target at $t_d = 55$ seconds while maintaining the look angle within the FOV limit, $\sigma_{\text{lim}} = 60$ deg. For comparison, guidance laws based on approximate time-to-go is considered that are summarized in Table 2. To exclude the sources of trajectory variation other than the time-to-go relation used in the comparative study, the guidance commands in Refs. (Zhang et al. 2014) and (He et al. 2020) are modified so that the error dynamics follow the following form that is similar to Eq. (32).

$$\dot{e}_t + K_e sgn(e_t) \left(\frac{|e_t|}{|e_t(0)|} \right)^{\alpha} = 0 \tag{77}$$

Figure 4 shows the simulation results of the scenario 2. The missile is required to increase the flight time to achieve the desired impact time, and therefore, the look angle increases until it reaches the limit value. As shown in Figs. 4d- 4b, all guidance laws regulate the time-to-go error while the look angle remained within the FOV. To satisfy the look angle constraint, each guidance law exhibits slightly different behavior, which can be attributed to the different shaping functions. Note that the proposed guidance law uses f_1 as the shaping function, Eq. (76), which is less flat. The shaping function f_1 leads the look angle of the proposed guidance scheme to keep decreasing after it reaches its maximum value as shown in Fig. 4b. The shaping function used in Ref. (He et al. 2020) makes the look angle stay near the FOV for a longer period of time, which is advantageous for faster convergence of the impact time error as compared to other schemes. After the time-to-go error vanishes, the baseline guidance law, PPNG, allows the missile to complete the flight. However, it is observed that the guidance commands using the approximated formulae become divergent near the interception. It is clear that the approximate time-to-go cannot be perfectly compensated for the effect of the approximation error due to the truncation and small angle assumption. Although the time-to-go error defined with respect to an approximate expression for the time-to-go vanishes, the actual time-to-go may still be nonzero, leading to potential instabilities near the end of the engagement.

5.3 Scenario 3: Comparison Between Proposed Guidance Laws

In the last scenario, the performance of the proposed guidance laws are compared. In this simulation, the missile autopilot dynamics is considered as a first-order lag system with a time constant $\tau = 0.1$ s. Two different values are considered for the desired impact time, i.e., $t_d = 45$ and 50 seconds. Table 4 summarizes the simulation cases for scenario 3. For a fair comparison, design parameters for the guidance laws $a_{bias,2}$ and $a_{bias,2a}$ are chosen in accordance with Eq. (68). For quantitative comparison of the proposed guidance laws, an average energy consumption is considered as the performance index.

$$J_{energy} = \frac{1}{t_f} \int_{t_0}^{t_f} a_m^2(t) dt, \tag{78}$$

Figure 5 shows the simulation results for the scenario 3. The proposed guidance laws generate smooth guidance commands to achieve the look angle constraint and impact time as shown in Fig. 5e. Despite the time-lag response induced by the autopilot, the proposed guidance laws show satisfactory performance for the impact time and miss distance. The feedback routine based on the exact time-to-go in the proposed guidance laws provide improved robust performance against autopilot delay compared to the existing open-loop type methods. It is shown that the guidance laws $a_{bias,1}$ and $a_{bias,2}$ present similar responses as discussed in Sec. 4.3. Compared to the guidance law 1, the missile using $a_{bias,2}$ maintains the look angle near the limit for a longer time, because the feedback command for the look angle is reduced when approaching its limit value. It is also observed that the reference modification in the second method, using $a_{bias,2a}$ shows different response compared to two guidance laws. The look angle profile tracks the limit value until the time-to-go error vanishes, and the guidance command shows a relatively abrupt transition after the error regulation, which is similar to two-stage guidance laws (Lee et al. 2020). This behavior leads to stable interception near collision and would produce much wider range of achievable impact time. Table 4 summarizes the simulation results. The proposed guidance methods achieve precise impact time and small miss distance. Relatively, the guidance law 1 shows accurate impact time precision, and guidance law 2a is effective judged by overall performance measures J_{energy}, miss distance, and time-to-go error.

6 CONCLUSION

This study proposed new biased proportional navigation guidance laws via analytic approach for impact-time-control under look angle constraints. The proposed guidance laws utilized the exact time-to-go solution of the proportional navigation guidance to maintain the performance advantages of the baseline guidance law near the end of engagement. The proposed guidance schemes based on both direct and indirect control of the time-to-go error achieved satisfactory impact time performance while also satisfying the look angle constraint. Furthermore, the proposed schemes demonstrated higher accuracy in impact-time-control compared to existing methods that rely on approximate time-to-go expressions. Overall, the proposed guidance laws provide a promising

approach to achieve precise impact-time-control under look angle constraints, which can be further extended to cooperative guidance problem of multiple missiles.

DATA AVAILABILITY STATEMENT

Some or all data, models, or code that support the findings of this study are available from the corresponding author upon reasonable request.

ACKNOWLEDGMENTS

This work was supported by the Chung-Ang University Research Grants in 2023 and the National Research Foundation of Korea(NRF) grant funded by the Korea government(MSIT) (No. RS-2023-00251551).

REFERENCES

Chen, X. and Wang, J. (2018). "Nonsingular Sliding-Mode Control for Field-of-View Constrained Impact Time Guidance." *Journal of Guidance, Control, and Dynamics*, 41(5), 1210–1218.

Cho, D., Kim, H. J., and Tahk, M. J. (2016). "Nonsingular Sliding Mode Guidance for Impact Time Control." *Journal of Guidance, Control, and Dynamics*, 39(1), 61–68.

Cho, N. and Kim, Y. (2016). "Modified Pure Proportional Navigation Guidance Law for Impact Time Control." *Journal of Guidance, Control, and Dynamics*, 39(4), 852–872.

Cho, N. and Lee, S. (2021). "Look-angle-constrained control of arrival time with exact knowledge of time-to-go." *Journal of Guidance, Control, and Dynamics*, 44(10), 1902–1908.

Dhananjay, N. and Ghose, D. (2014). "Accurate Time-to-Go Estimation for Proportional Navigation Guidance." *Journal of Guidance, Control, and Dynamics*, 37(4), 1378–1383.

Dong, W., Wang, C., Wang, J., Son, H., and Xin, M. (2022). "Unified method for field-of-view-limited homing guidance." *Journal of Guidance, Control, and Dynamics*, 45(8), 1415–1434.

Dong, W., Wang, C., Wang, J., and Xin, M. (2023). "Varying-gain proportional navigation guidance for precise impact time control." *Journal of Guidance, Control, and Dynamics*, 46(3), 535–552.

Erer, K. S. and Tekin, R. (2016). "Impact Time and Angle Control Based on Constrained Optimal Solutions." *Journal of Guidance, Control, and Dynamics*, 39(10), 2445–2451.

Gasper, G., Rahman, M., and George, G. (2004). *Basic Hypergeometric Series*, Vol. 96. Cambridge University Press, Cambridge, UK.

Harl, N. and Balakrishnan, S. N. (2012). "Impact Time and Angle Guidance with Sliding Mode Control." *IEEE Transactions on Control Systems Technology*, 20(6), 1436–1449.

Harrison, G. A. (2012). "Hybrid Guidance Law for Approach Angle and Time-of-Arrival Control." *Journal of Guidance, Control, and Dynamics*, 35(4), 1104–1114.

He, S., Lee, C.-H., Shin, H.-S., and Tsourdos, A. (2020). *Optimal Guidance and Its Applications in Missiles and UAVs*. Springer, Gewerbestr, Switzerland.

Hu, Q., Han, T., and Xin, M. (2018). "New Impact Time and Angle Guidance Strategy via Virtual Target Approach." *Journal of Guidance, Control, and Dynamics*, 41(8), 1755–1765.

Hu, Q., Han, T., and Xin, M. (2019). "Sliding-mode impact time guidance law design for various target motions." *Journal of Guidance, Control, and Dynamics*, 42(1), 136–148.

Jeon, I. S. and Lee, J. I. (2017). "Impact-Time-Control Guidance Law with Constraints on Seeker Look Angle." *IEEE Transactions on Aerospace and Electronic Systems*, 53(5), 2621–2627.

Jeon, I. S., Lee, J. I., and Tahk, M. J. (2006). "Impact-Time-Control Guidance Law for Anti-Ship Missiles." *IEEE Transactions on Control Systems Technology*, 14(2), 260–266.

Jeon, I. S., Lee, J. I., and Tahk, M. J. (2010). "Homing Guidance Law for Cooperative Attack of Multiple Missiles." *Journal of Guidance, Control, and Dynamics*, 33(1), 275–280.

Kang, H., Wang, P., and Song, S. (2023a). "A generalized three-dimensional cooperative guidance law for various communication topologies with field-of-view constraint." *Proceedings of the Institution of Mechanical Engineers, Part G: Journal of Aerospace Engineering*, 09544100231153265.

Kang, H., Wang, P., Wei, S., and Song, S. (2023b). "Three-dimensional impact-time-constrained proportional navigation guidance using range-varying gain." *Aerospace Science and Technology*, 108419.

Khalil, H. K., and Grizzle, J. W. (1996). *Nonlinear Systems*, Vol. 3. Prentice hall, Upper Saddle River, NJ.

Kim, H. G., Cho, D., and Kim, H. J. (2019a). "Sliding Mode Guidance Law for Impact Time Control without Explicit Time-to-go Estimation." *IEEE Transactions on Aerospace and Electronic Systems*, 55(1), 236–250.

Kim, H. G. and Kim, H. J. (2019). "Backstepping-based Impact Time Control Guidance Law for Missiles with Reduced Seeker Field-of-View." *IEEE Transactions on Aerospace and Electronic Systems*, 55(1), 82–94.

Kim, H.-G., Lee, J.-Y., Kim, H. J., Kwon, H.-H., and Park, J.-S. (2020). "Look-Angle-Shaping Guidance Law for Impact Angle and Time Control with Field-of-View Constraint." *IEEE Transactions on Aerospace and Electronic Systems*, 56(2), 1602–1612.

Kim, J., Cho, N., and Kim, Y. (2019b). "Field-of-view constrained impact angle control guidance guaranteeing error convergence before interception." *AIAA Scitech 2019 Forum*, 1927.

Kim, J., Cho, N., and Kim, Y. (2021). "Field-of-view-constrained impact angle control guidance with error convergence before interception considering speed changes." *Proceedings of the Institution of Mechanical Engineers, Part G: Journal of Aerospace Engineering*, 235(2), 238–256.

Kim, M., Jung, B., Han, B., Lee, S., and Kim, Y. (2015). "Lyapunov-based Impact Time Control Guidance Laws Against Stationary Targets." *IEEE Transactions on Aerospace and Electronic Systems*, 51(2), 1111–1122.

Kim, T.-H., Lee, C.-H., Jeon, I.-S., and Tahk, M.-J. (2013). "Augmented Polynomial Guidance with Impact Time and Angle Constraints." *IEEE Transactions on Aerospace and Electronic Systems*, 49(4), 2806–2817.

Kumar, S. R. and Ghose, D. (2015). "Impact Tme Guidance for Large Heading Errors Using Sliding Mode Control." *IEEE Transactions on Aerospace and Electronic Systems*, 51(4), 3123–3138.

Lee, J. I., Jeon, I. S., and Tahk, M. J. (2007). "Guidance Law to Control Impact Time and Angle." *IEEE Transactions on Aerospace and Electronic Systems*, 43(1), 301–310.

Lee, S., Cho, N., and Kim, Y. (2020). "Impact-Time-Control Guidance Strategy with a Composite Structure Considering the Seeker's Field-of-View Constraint." *Journal of Guidance, Control,*

675 *and Dynamics*, 43(8), 1566–1574.

676 Levant, A. (2001). "Universal Single-Input-Single-Output (SISO) Sliding-Mode Controllers with
677 Finite-Time Convergence." *IEEE transactions on Automatic Control*, 46(9), 1447–1451.

678 Li, Z. and Ding, Z. (2018). "Robust Cooperative Guidance Law for Simultaneous Arrival." *IEEE*
679 *Transactions on Control Systems Technology*, 27(3), 1360–1367.

680 Livermore, R. and Shima, T. (2018). "Deviated Pure-Pursuit-Based Optimal Guidance Law for
681 Imposing Intercept Time and Angle." *Journal of Guidance, Control, and Dynamics*, 41(8),
682 1807–1814.

683 Lozier, D. W. (2003). "Nist digital library of mathematical functions." *Annals of Mathematics and*
684 *Artificial Intelligence*, 38, 105–119.

685 Pearson, J. W. (2009). "Computation of hypergeometric functions." Ph.D. thesis, University of
686 Oxford, University of Oxford.

687 Ryoo, C.-K., Cho, H., and Tahk, M.-J. (2006). "Time-to-go Weighted Optimal Guidance with
688 Impact Angle Constraints." *IEEE Transactions on Control Systems Technology*, 14(3), 483–492.

689 Saleem, A. and Ratnoo, A. (2016). "Lyapunov-based Guidance Law for Impact Time Control and
690 Simultaneous Arrival." *Journal of Guidance, Control, and Dynamics*, 39(1), 164–172.

691 Sang, D. K. and Tahk, M. J. (2009). "Guidance Law Switching Logic Considering the Seeker's
692 Field-of-View Limits." *Proceedings of the Institution of Mechanical Engineers, Part G: Journal*
693 *of Aerospace Engineering*, 223(8), 1049–1058.

694 Shneydor, N. A. (1998). *Missile Guidance and Pursuit: Kinematics, Dynamics and Control*.
695 Woodehead, Cambridge, UK.

696 Shtessel, Y. B., Shkolnikov, I. A., and Levant, A. (2007). "Smooth Second-Order Sliding Modes:
697 Missile Guidance Application." *Automatica*, 43(8), 1470–1476.

698 Tahk, M. J., Shim, S. W., Hong, S. M., Choi, H. L., and Lee, C. H. (2018). "Impact Time Control
699 Based on Time-to-Go Prediction for Sea-Skimming Antiship Missiles." *IEEE Transactions on*
700 *Aerospace and Electronic Systems*, 54(4), 2043–2052.

701 Tekin, R. and Erer, K. S. (2020). "Impact Time and Angle Control Against Moving Targets with

Look Angle Shaping." *Journal of Guidance, Control, and Dynamics*, 43(5), 1020–1025.

Tekin, R., Erer, K. S., and Holzapfel, F. (2016). "Control of Impact Time with Increased Robustness via Feedback Linearization." *Journal of Guidance, Control, and Dynamics*, 39(7), 1682–1689.

Tekin, R., Erer, K. S., and Holzapfel, F. (2017a). "Adaptive Impact Time Control via Look-Angle Shaping under Varying Velocity." *Journal of Guidance, Control, and Dynamics*, 40(12), 3247–3255.

Tekin, R., Erer, K. S., and Holzapfel, F. (2017b). "Polynomial Shaping of the Look Angle for Impact-Time Control." *Journal of Guidance, Control, and Dynamics*, 40(10), 2666–2671.

Tekin, R., Erer, K. S., and Holzapfel, F. (2018). "Impact Time Control with Generalized-Polynomial Range Formulation." *Journal of Guidance, Control, and Dynamics*, 41(5), 1190–1195.

Tsalik, R. and Shima, T. (2019). "Circular Impact-Time Guidance." *Journal of Guidance, Control, and Dynamics*, 42(8), 1836–1847.

Wang, P., Guo, Y., Ma, G., and Wie, B. (2019). "New Differential Geometric Guidance Strategies for Impact-Time Control Problem." *Journal of Guidance, Control, and Dynamics*, 42(9), 1982–1992.

Zarchan, P. (2012). *Tactical and Strategic Missile Guidance*. American Institute of Aeronautics and Astronautics, Inc., Reston, VA.

Zhang, S., Guo, Y., Liu, Z., Wang, S., and Hu, X. (2020). "Finite-Time Cooperative Guidance Strategy for Impact Angle and Time Control." *IEEE Transactions on Aerospace and Electronic Systems*.

Zhang, Y., Wang, X., and Wu, H. (2014). "Impact Time Control Guidance Law with Field of View Constraint." *Aerospace Science and Technology*, 39, 361–369.

List of Tables

1 Simulation Cases of Scenario 1 35

2 Time-to-Go and Guidance Commands 36

3 Summary of Simulation Results (Scenario 2) 37

4 Simulation Cases of Scenario 3 and Summary of Results 38

TABLE 1. Simulation Cases of Scenario 1

Parameter	Case 1-1	Case 1-2	Case 1-3	Case 1-4	Case 1-5	Case 1-6
Shaping function	$f_1(\sigma)$	$f_1(\sigma)$	$f_1(\sigma)$	$f_2(\sigma)$	$f_2(\sigma)$	$f_2(\sigma)$
Exponent α	0.3	0.7	1	0.3	0.7	1

TABLE 2. Time-to-Go and Guidance Commands

Case	Time-to-Go	Guidance Command	Parameters
2-1	$t_{go,PPN}$	Eq. (30), with $f_1(\sigma)$ in Eq. (76)	$\alpha = 0.8$, $p = 8$
2-2	$t_{go,approx,small}$	$a = -\frac{K(2N-1)V^2}{r\sigma}\cos\left(\frac{\pi\sigma}{2\sigma_{\lim}}\right) sgn(e_t)\left(\frac{\lvert e_t\rvert}{\lvert e_t(0)\rvert}\right)^{\alpha}$	$\alpha = 0.8$, $K = 8$
2-3	$t_{go,approx}$	$a = -\frac{K(2N-1)V^2}{r\sin\sigma}\cos\left(\frac{\pi}{2}\left(\frac{\sigma}{\sigma_{\lim}}\right)^5\right) sgn(e_t)\left(\frac{\lvert e_t\rvert}{\lvert e_t(0)\rvert}\right)^{\alpha}$	$\alpha = 0.8$, $K = 8$

TABLE 3. Summary of Simulation Results (Scenario 2)

Performance Measures	Proposed	Ref. (Zhang et al. 2014)	Ref. (He et al. 2020)
Zero-effort-miss ($Z(t_f),\ [m]$)	$0.219 \cdot 10^{-7}$	0.016	0.022
Impact Time ($t_f,\ [s]$)	55.000	55.1012	55.1352

TABLE 4. Simulation Cases of Scenario 3 and Summary of Results

Parameters and Performance Measures	Case 3-1	Case 3-2	Case 3-3	Case 3-4	Case 3-5	Case 3-6
Guidance Law	1	1	2	2	$2a$	$2a$
Desired Impact Time (s)	45	50	45	50	45	50
zero-effort-miss (m)	0.005	0.013	0.289	0.490	0.001	0.001
Time-to-Go Error ($\lvert(t_f) - t_d\rvert$, $[10^{-3}s]$)	0.001	0.003	0.072	0.317	0.002	0.027
J_{energy} $[10^3 m^2/s^4]$	0.712	0.812	0.599	0.647	0.732	0.693

List of Figures

1 Engagement Geometry 40
2 Concept of Desired Look Angle and Reference Look Angle 41
3 Simulation Results for Scenario 1: Effects of Design Parameters 42
4 Simulation Results for Scenario 2: Comparison with Guidance Laws Based on Approximate Time-to-Go 43
5 Simulation Results for Scenario 3: Comparison Between Proposed Guidance Laws 44

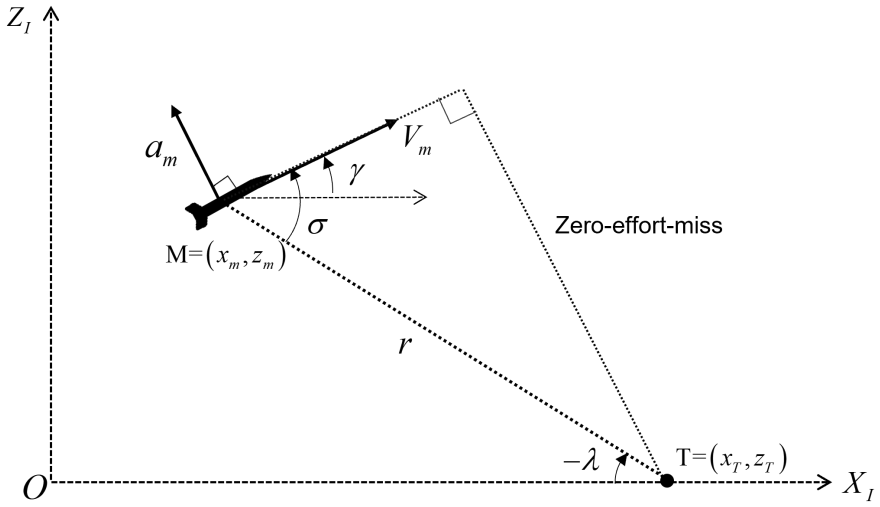


Fig. 1. Engagement Geometry

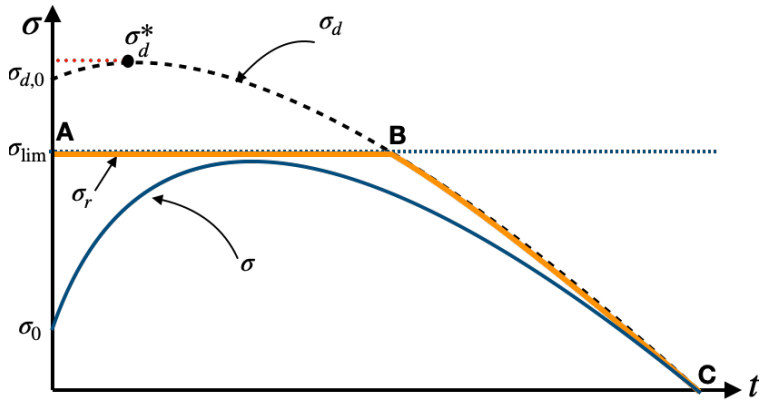
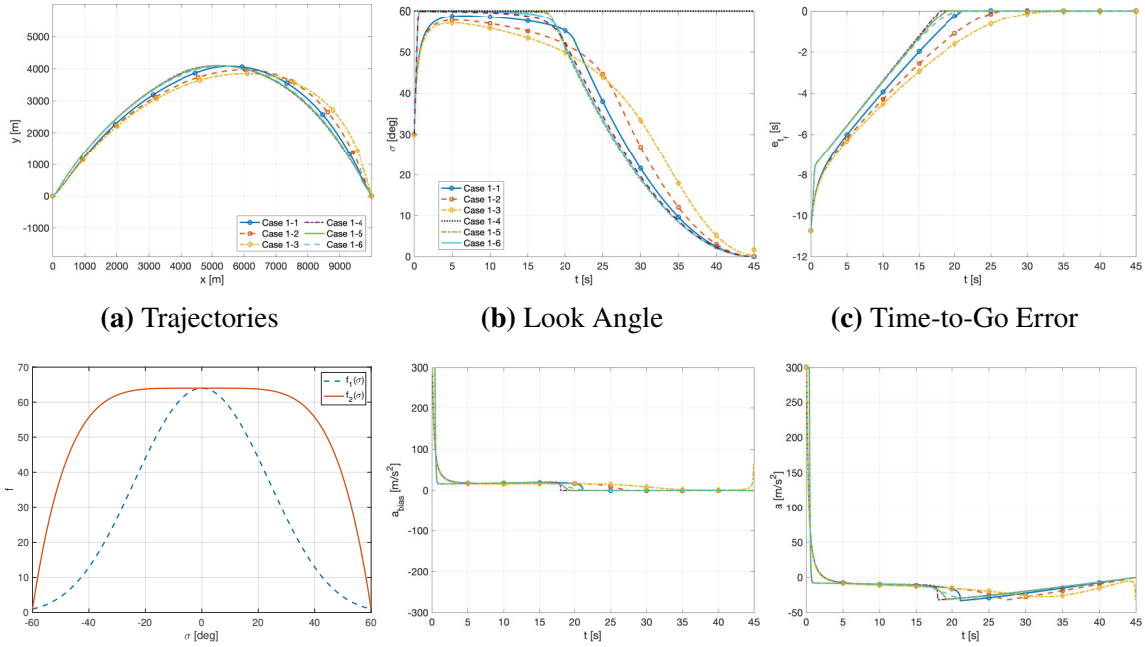


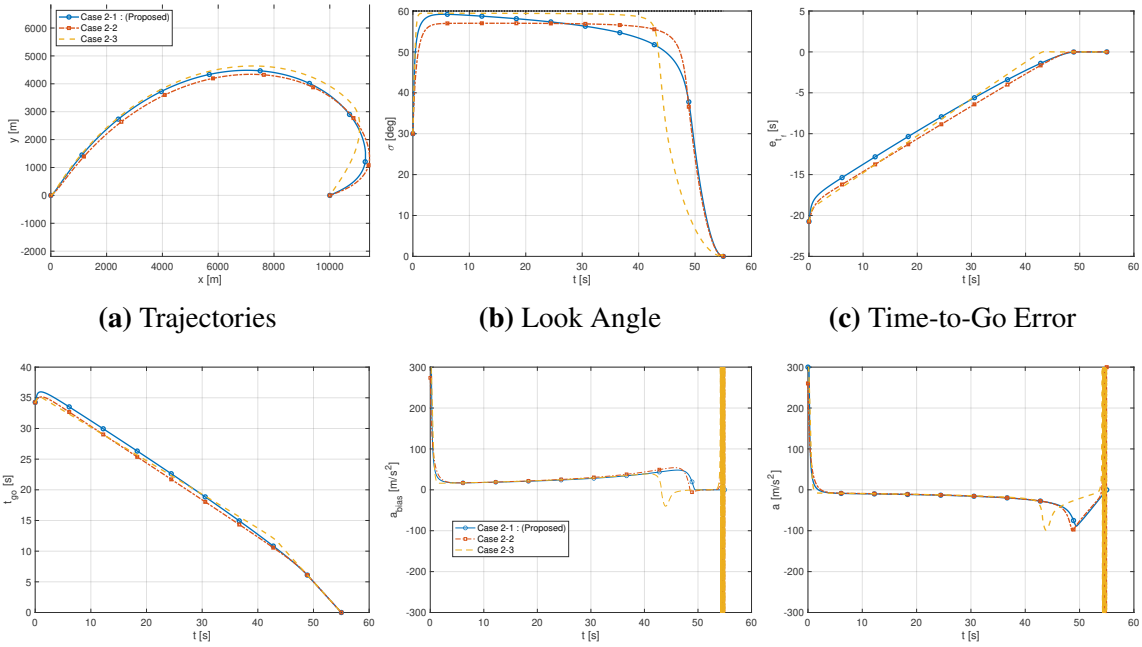
Fig. 2. Concept of Desired Look Angle and Reference Look Angle



(a) Trajectories **(b)** Look Angle **(c)** Time-to-Go Error

(d) Shaping Function **(e)** Bias Input **(f)** Acceleration

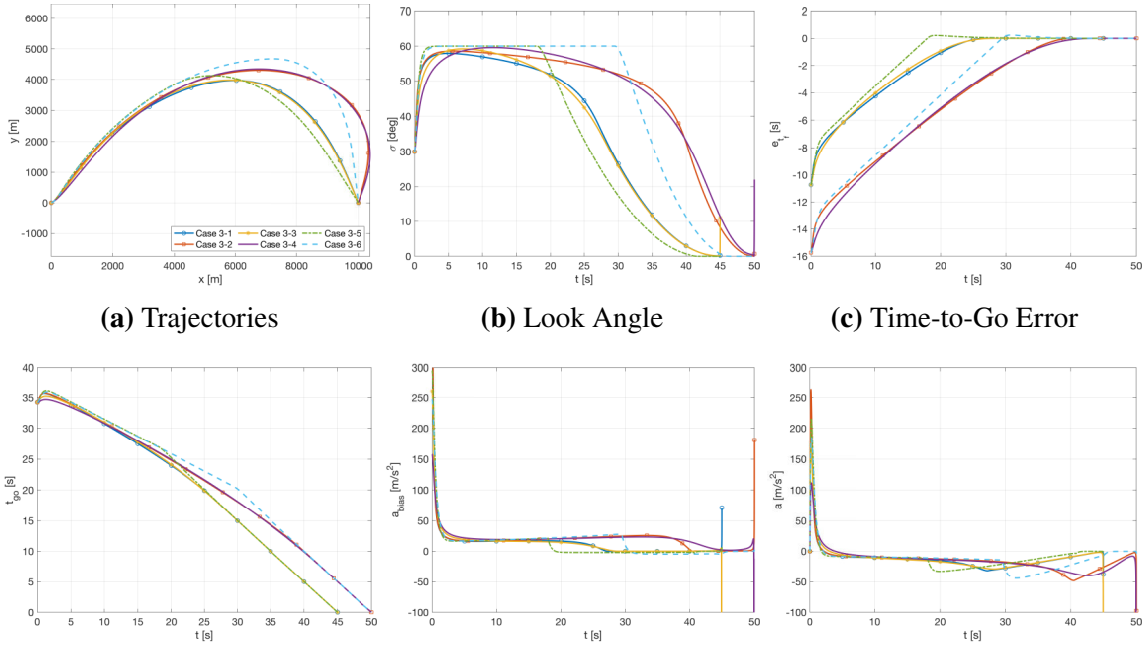
Fig. 3. Simulation Results for Scenario 1: Effects of Design Parameters



(a) Trajectories **(b)** Look Angle **(c)** Time-to-Go Error

(d) Time-to-Go **(e)** Bias Input **(f)** Acceleration

Fig. 4. Simulation Results for Scenario 2: Comparison with Guidance Laws Based on Approximate Time-to-Go



(a) Trajectories **(b)** Look Angle **(c)** Time-to-Go Error

(d) Time-to-Go **(e)** Bias Input **(f)** Acceleration

Fig. 5. Simulation Results for Scenario 3: Comparison Between Proposed Guidance Laws



https://dspace.org/

Analytic approach to impact time guidance with look angle constraint using exact time-to-go solution

Lee, Seokwon; Kim, Jinrae; Kim, Youdan; Cho, Namhoon

2024-03-01
American Society of Civil Engineers (ASCE)
https://doi.org/10.1061/JAEEEZ.ASENG-5250
Lee S, Kim J, Kim Y Cho N. (2024) Analytic approach to impact time guidance with look angle constraint using exact time-to-go solution. Journal of Aerospace Engineering, Volume 37, Issue 2, March 2024, Article number 5250

Downloaded from a DSpace repository. https://dspace.org/